

Proceeding Paper

Solvatochromic Behavior of Polarity Indicators in PILs and Their Mixtures with Molecular Solvents: Autoprotolysis and Its Relation to Acidity [†]

Claudia Guadalupe Adam , Lucía Gamba and Maria Virginia Bravo ^{*}

Laboratory of Organic Physicochemistry, Institute of Applied Chemistry of the Littoral (IQAL) (UNL-CONICET), Faculty of Chemical Engineering, University National of Litoral, Santa Fe CP3000, Argentina; cadam@fiq.unl.edu.ar (C.G.A.); lucীগamba455@gmail.com (L.G.)

^{*} Correspondence: mvbravo@fiq.unl.edu.ar; Fax: +54-342-4571-162

[†] Presented at the 25th International Electronic Conference on Synthetic Organic Chemistry, 15–30 November 2021; Available online: <https://ecsoc-25.sciforum.net/>.

Abstract: It is interesting to know the behavior of Protic Ionic Liquids (PILs) within the binary mixture of molecular solvents, since it is usual to carry out processes such as organic and inorganic synthesis, or liquid–liquid extractions in the presence of another solvent. Moreover, on certain occasions, the absence of water is strictly required. In this sense, it is important to note that the addition of small amounts of IL to the molecular solvent allows a fine adjustment in its microscopic properties, obtaining “new solvent systems” with particular properties. The solvatochromic dyes are traditionally used as microscopic descriptors to determine the molecular microscopic properties of solvents, so we aim to re-evaluate the behavior of these probes and reconsider the validity of traditional polarity scales such as $E_T(30)$ in alkylammonium-based PILs, as well as in their mixtures with molecular solvents, knowing that the real composition of these PILs depends on the equilibrium of autoprotolysis. The characterization of systems was completed in terms of a change in the ΔpK_a of the precursor species of a PIL. A thermal analysis was also employed to determine the acid strength’s role in an ion’s complete formation in pure PILs.

Keywords: Protic Ionic Liquids; solvatochromic indicators; equilibrium of autoprotolysis



Citation: Adam, C.G.; Gamba, L.; Bravo, M.V. Solvatochromic Behavior of Polarity Indicators in PILs and Their Mixtures with Molecular Solvents: Autoprotolysis and Its Relation to Acidity. *Chem. Proc.* **2022**, *8*, 92. <https://doi.org/10.3390/ecsoc-25-11746>

Academic Editor: Julio A. Seijas

Published: 14 November 2021

Publisher’s Note: MDPI stays neutral with regard to jurisdictional claims in published maps and institutional affiliations.



Copyright: © 2021 by the authors. Licensee MDPI, Basel, Switzerland. This article is an open access article distributed under the terms and conditions of the Creative Commons Attribution (CC BY) license (<https://creativecommons.org/licenses/by/4.0/>).

1. Introduction

Ionic liquids (ILs) have a great advantage over other types of solvents because of the wide versatility that they present with different applications (especially for electrochemical applications), due to their physicochemical properties, such as high ionic conductivity [1–12]. For this reason, they are called the ‘new materials’. In general, ILs can be classified into Protic ILs (PILs) and Aprotic ILs (AILs). PILs are a kind of IL, formed by the proton transfer from a Brønsted acid (AH) to a Brønsted base (B) [13,14]. One of the structural features of PILs is the formation of strong H bonds between cations and anions that define their unique physicochemical properties [15–17]. We have determined by cyclic voltammetry that neutral acidic and basic precursor species can coexist in PILs because of the equilibrium of autoprotolysis [18], which can affect its properties, such as viscosity, density, and conductivity.

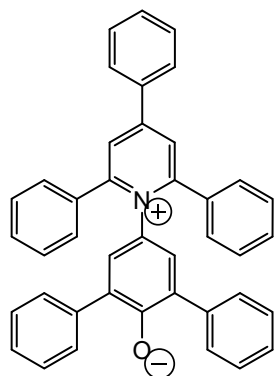
Additionally, it is interesting to know the behavior of PILs within the binary mixture of molecular solvents, since it is usual to carry out certain processes such as organic and inorganic synthesis or liquid–liquid extractions in the presence of a second solvent. Moreover, on certain occasions the absence of water is strictly required. In this sense, it is important to mention that the addition of small amounts of IL to molecular solvent allows the optimization of its microscopic properties, obtaining “new solvent systems” [19,20]. Taking into account that solvatochromic indicators are traditionally used as microscopic

descriptors to determine the molecular microscopic properties of solvents, [21] we aim to re-evaluate the behavior of solvatochromic probes and reconsider the validity of traditional polarity scales such as $E_T(30)$ [22,23] in alkylammonium-based PILs and in their mixtures with molecular solvents, knowing that the real composition of these PILs depends on the equilibrium of autoprotolysis.

We have detected certain challenges in the last years when working with IL, such as the effects of different acid-base equilibria between the free precursor species of the PILs and these indicators. Thus, the parameters that are obtained by these scales would be contaminated and would not represent reliable results within the normalized values that constitute the scales. This is also a problem, since the solvents that are used to construct these scales are molecular and do not involve ionic species. Complementing this, some authors [24] establish that it is possible to discuss the physicochemical properties in terms of a change in the ΔpK_a of the precursor species of a PIL, in order to analyze the degree of proton transfer and thermal stability as a function of the change in the ΔpK_a . In addition, thermal analyses are employed to relate the degree of the acidity in an ion's complete formation in pure PILs.

2. Materials and Methods

For the analysis, we have selected Reichardt's dye (I) (Scheme 1) and the PILs: ethylammonium nitrate (NEA); diethylammonium nitrate (NDEA); and tributylammonium nitrate (NTBA), and the chemical precursors of the PILs are: ethylamine, diethylamine, tributylamine, and nitric acid.



Scheme 1. Structure of the Reichardt's dye (I): betaine 2,6-diphenyl-4-(2,4,6-triphenyl-1-pyridinium)-1-phenolate.

The molecular solvents are methanol (MeOH) with hydrogen bond donor (HBD) and hydrogen bond acceptor (HBA) properties, and dimethylsulfoxide (DMSO) with HBA properties.

The response of the indicators was analyzed for different ranges of concentrations of the PILs in the binary mixtures (molar concentrations (C(M)) and molar fractions (x)), in order to evaluate the solvation effect of molecular solvents.

2.1. Synthesis of Ionic Liquids

The investigated PILs were synthesized, as detailed in the literature [8].

2.2. Microsensors and Spectroscopic Behavior—UV-Vis Spectroscopy

General Procedure: The spectroscopic data were obtained with a SHIMADZU UV-1800 spectrophotometer, equipped with a thermostatic cell holder. The pure solvents were mixed in appropriate proportions by weight to give binary solvent mixtures at different compositions. The temperature was maintained at 25 ± 0.1 °C. The concentrations of the indicators solutions were: 0.1 and 0.25 mM for the Reichardt's dye (I).

The parameter $E_T(30)$ was determined from the wavelength corresponding to the maximum of the UV-Vis absorption band of betaine (I) and calculated by Equation (1):

$$E_T(30) \left[\text{kcal} \cdot \text{mol}^{-1} \right] = hc\tilde{\nu}N = 2.859 \times 10^{-3} \tilde{\nu} \left(\text{cm}^{-1} \right) \quad (1)$$

where h is Planck's constant, c is the speed of light, N is Avogadro's number, and n is the wave number in cm^{-1} . This equation relates the electronic transition in the probe to the corresponding intramolecular charge transfer energy in kcal/mol.

2.3. Thermogravimetric Analysis (TGA)

The decomposition temperatures (T_d) of the PILs were determined by using a thermogravimetric analyzer (TGA) in the thermal stability analysis [25–29]. An approximate 10 mg of sample was weighted in a crucible pan and the analysis was performed in the temperature range of 30–650 °C under 20 mL/min of nitrogen flow with a heating rate of 10 °C/min.

3. Results and Discussion

3.1. Solvatochromic Behavior of the Reichardt's Dye (I)

3.1.1. Range of Mole Fractions (x)

Figure 1 shows that there are no significant changes in the spectrum from $x_{\text{PIL}} \sim 0.2$ to 1 for dye I, which is sensitive to polarity and acidity. This possibly indicates that the ionic lattice is organized, and as a consequence, the solvation effect of the molecular solvent is negligible.

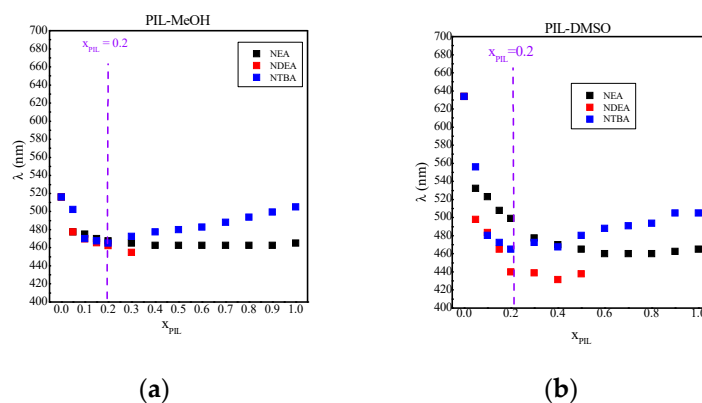


Figure 1. Variation of λ (nm) of I vs. the x_{PIL} in the mixtures: (a) (MeOH + PIL) y (b) (DMSO + PIL). (■ NEA, ■ NDEA, ■ NTBA).

Taking as a reference the observed behavior of NTBA by cyclic voltammetry, [8] where NO free molecular species were detected for this PIL in its pure state, we can associate the behavior of the probe with molar fractions that are close to 1 ($x_{\text{PIL}} \sim 1$) as an indicator of a microenvironment ionic polar.

Clearly, from $x_{\text{PIL}} \sim 0.2$ to 1, the interaction with dye I is governed by the ion pair of the PILs, independently of the molecular solvent, as shown in Figure 2 for NEA and NTBA. This would also indicate that the effect of ionic species on the probe prevails and not the mixed solvent (SM) or the PIL-SM intersolvent complex. This comparison could not be made for NDEA due to its limited solubility in the molecular solvents that were compared.

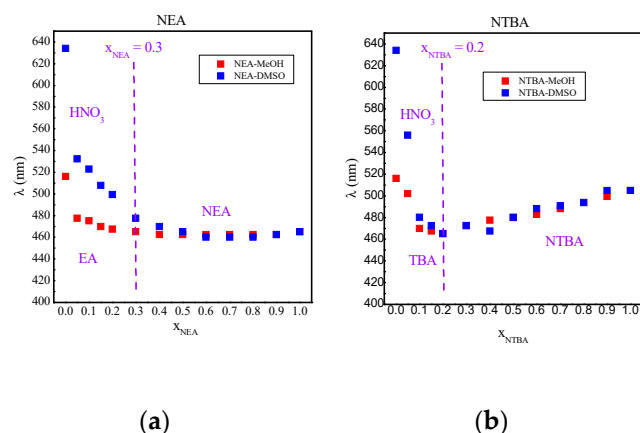


Figure 2. Variation of the λ (nm) of the indicator I vs. the x_{LI} for NEA and NTBA in: (a) ■ MeOH y (b) ■ DMSO.

On the other hand, we observe a shift to lower values of λ as the PIL concentration increases for lower molar fractions of the PIL in the range $0 < x < 0.3$. This could indicate that initially there are higher concentrations of free molecular species in the equilibrium of autoprotolysis due to a greater solvation effect by the molecular solvents that are found in a higher proportion.

3.1.2. Solvatochromic Behavior of Dye I in the Range of Mole Fractions

Figure 3 shows the response patterns of the factor $E_T(30)$ as a function of the x_{LI} for all the solvent systems under study. The analysis was developed according to the deviation from the ideality of the curves “property vs. solvent composition”.

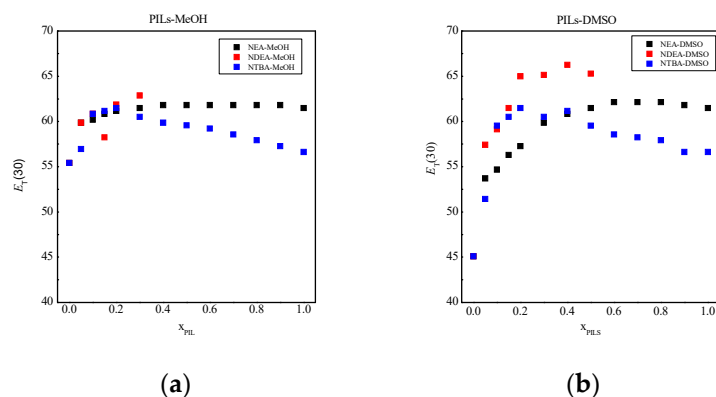


Figure 3. Variation of parameter $E_T(30)$ vs. x_{PIL} in mixtures: (a) (MeOH + PIL) y (b) (DMSO + PIL). (■ NEA, ■ NDEA, ■ NTBA).

Generally, in this study, the same response pattern could be observed for the $E_T(30)$ parameter (Figure 3). This observation could be related to the possibility of forming PIL–SM complexes. This possibility produces ionic species with different degrees of association in respect to the Pure PIL. The highest percentage of change in the properties was observed up to a value of $x_{PILs} \sim 0.2$.

It could also be noted that certain solvent systems showed synergism on the parameter and other mixtures showed positive deviation with respect to the ideal behavior. This property depends on the cation; for example, for NTBA, synergism was observed with the solvents MeOH and DMSO. In this case, we can associate the lowest polarity values $E_T(30)$ corresponding to a microenvironment with high ionic character when $x_{NTBA} \sim 1$.

From the analysis of the solvatochromic scales, we deem that it would not be appropriate to analyze the values of a normalized $E_T(30)$ parameter (E_T^N), since ionic organic

compounds are not involved in the normalization calculation. If it has a series of $E_T(30)$ values for several LIs, a new scale could be proposed.

3.1.3. Range of Molar Concentration (C) vs. x

In this study, the same behavior was observed in both solvents. We observed the protonation of the indicator by the acidic species precursor of the PILs in each solvent system for the C (M) range. However, surprisingly, we have detected that the indicator's band returns as a shoulder in all binary solvent mixtures of type [PILs + Molecular Solvent] here studied, when the I microsensor concentration is about 0.4 mM and the PILs concentration in the binary mixture is the order molar fraction. Figure 4 shows the behavior of Reichardt's dye (I) for the ([NDEA] + MeOH/DMSO) system binary for both ranges of working concentrations. This system was taken as a model, but similar behaviors were observed for all the binary systems here studied.

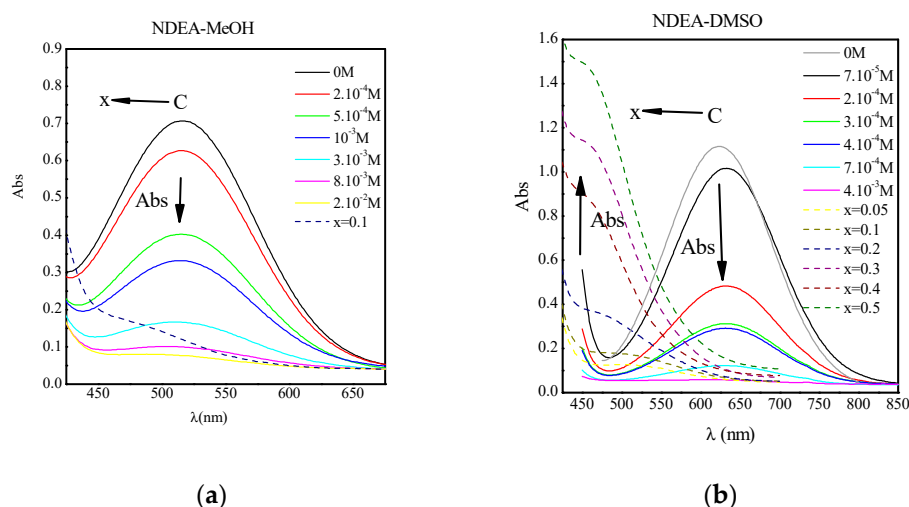


Figure 4. The UV/Vis absorption spectra of Reichardt's dye dissolved for (a) $[I] = 4 \times 10^{-4}$ M in MeOH, after addition of increasing amounts of [NDEA] in concentration (mol L^{-1}) (—) and mole fraction (---). (b) $[I] = 2.5 \times 10^{-4}$ M in DMSO, after addition of increasing amounts of [NDEA] in concentration (mol L^{-1}) and mole fraction.

The behavior of the probe in the presence of PILs in the range of molar concentrations is manifested as an indicator signal that turns off. This is clearly due to the presence of free acid in the medium and the consequent protonation of the indicator that absorbs at lower wavelengths.

When the [PILs] is in molar fraction, the dye signal returns to 'switching-on'. At first, this unexpected behavior could, in principle, be explicated through the equilibrium of autoprotolysis at different amounts of PILs.

3.2. ΔpK_a

Some authors have analyzed the physicochemical properties in terms of a change in the ΔpK_a of its precursor species ($\Delta pK_a^{\text{solvent}} = pK_a^{\text{AmH}^+/\text{B}} - pK_a^{\text{HA}/\text{A}}$) [14]. They have also analyzed the applicability of the relationships between different parameters with the ΔpK_a of the PILs to establish a generalized concept, in order to understand the physicochemical properties. In this analysis, special emphasis is given to the degree of proton transfer and thermal stability depending on the change in the ΔpK_a . Based on the above, we may find some relationship in molecular solvents between the parameters that are determined in our work and the ΔpK_a of the PILs that are analyzed here. Consequently, we could be able to analyze the degree of ion pair formation that these PILs present in MeOH and DMSO, in order to apply them to non-aqueous systems. This is important because most of the reported data were obtained in aqueous systems.

In addition, Angell et al. specifically demonstrated that an ΔpK_a of >10 is required to ensure sufficient proton transfer to produce highly ionized PILs [30]. So, if the PILs have a high ΔpK_a , then their ionic behavior will be high as well. This may indicate complete proton transfer and weaker interactions between the cation and the anion. However, MacFarlane et al. proposed that $\Delta pK_a = 4$ is sufficient for the completion of proton transfer [31]. ILs with lower ΔpK_a values indicate incomplete proton transfer and the formation of ion-pairs or ion-aggregates between the protonated cation and the anion, similar to AILs [32]. These PILs with a low ΔpK_a exhibit poor ionic behavior, indicating the hydrogen bonding interaction between the cation and the anion through the N–H bond as a result of an incomplete proton transfer [24].

Knowing the above, we can compare the ΔpK_a of the PILs in MeOH and DMSO (Table 1).

Table 1. Calculated ΔpK_a values for PILs in MeOH and DMSO. pK_a values of amines and HNO_3 in MeOH, DMSO and water were taken from reference [33–37].

Species	pK_a^w	pK_a^{MeOH}	pK_a^{DMSO}	ΔpK_a^w	ΔpK_a^{MeOH}	ΔpK_a^{DMSO}
HNO_3	−1.3	3.18	−1.72		Am/ HNO_3	
EA	10.63	11.00	10.90	11.93	7.82	12.62
DEA	10.98	11.00	10.50	12.28	7.82	12.22
TBA	10.89	10.78	8.4	12.19	7.60	10.12

We obtained an $\Delta pK_a > 10$ for the PILs in water and DMSO, which indicates a sufficient proton transfer to produce a PIL with a high ionic character, while in MeOH, the character of the IL as an ionic pair is evidently lower. This is consistent with the highest $E_T(30)$ values that are obtained for the MeOH solvent in the range of x_{PILs} between 0 and 0.2, corresponding to a poor ionic character. The above also agrees with the lower value of pK_a that is determined by the indicator method (Table 2) in MeOH in respect to DMSO, due to the greater dissociation of the PILs in MeOH generating free HNO_3 . We could corroborate the high degree of ionization that is observed in DMSO by comparing the pK_a values of HNO_3 (Table 1), being more acidic in DMSO. However, these PILs with high pK_a values showed low amounts of free acid in this solvent.

Table 2. Acidity constants for selected PILs in MeOH and DMSO [21].

PILs	pK_a^{PIL}	
	MeOH	DMSO
NEA	5.38	8.67
NDEA	5.21	7.87
NTBA	4.34	6.33
pK_a^{dye}	5.10	8.90

The previously published pK_a values show that in DBH solvents, such as MeOH, there is a shift from the equilibrium of autoprotolysis towards molecular species, while DBH solvents such as DMSO cause the opposite effect, favoring the existence of PILs mainly as ionic pairs.

Some authors propose that PILs with weaker bases are poor ionic liquids [38–41]. If we compare the different cations EA, DEA, and TBA for the same acid, we corroborate that for the strongest amine with TBA as a base, the PILs with the highest ionic character are obtained in the pure state. However, the presence of molecular solvents modifies this fact due to the solvation effect, with NTBAs being the most acidic PILs in both solvents.

3.3. TGA

Some authors have established that strong hydrogen bonds between the cation and anion are present in PILs through N–H bonds, in addition to inter-ionic interactions such

as Coulombic interactions and van der Waals forces, which are seen in aprotic ionic liquids (AILs) [42–44]. Furthermore, they have demonstrated that the bond strength may vary by changing the structure and strength of the constituent acids and bases of the PILs. The successive breaking of hydrogen bonds with temperature explains the characteristic properties of PILs, such as a relatively low ionic character and its decrease with temperature [45]. In this sense, the study of the thermal analysis of a substance is crucial, as it provides information on the behavior of a compound with the variation of the temperature.

The thermal stability of the PIL was examined by a thermogravimetric analysis (TGA), and the TGA profiles are graphically presented in Figure 5. The TGA was performed at scanning rate of 10 °C/min. In the TGA study, the main factor of thermal stability depends on the strength of the heteroatom–carbon and heteroatom–hydrogen bond [46].

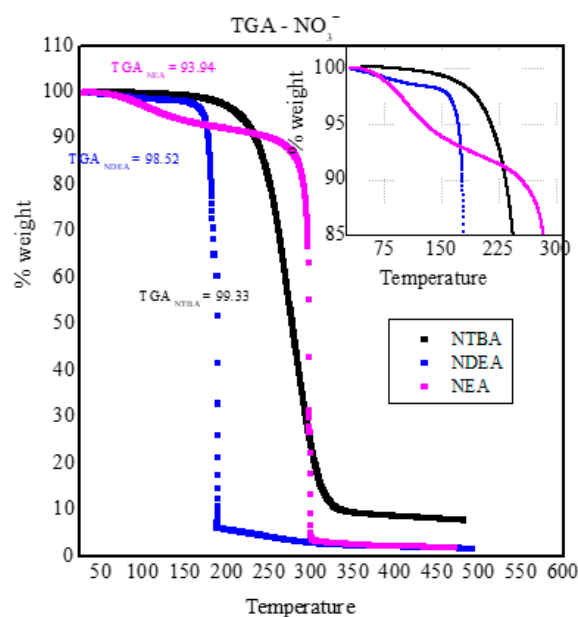


Figure 5. TG curves of PILs recorded at 10 °C/min for NEA, NDEA, and NTBA.

The T_d (decomposition temperature) was determined as the initial temperature at which weight loss began in the TGA analysis, also called the initial decomposition. All the data were fitted using the Boltzmann equation. Figure 5 shows the results that were obtained in TGA for PILs.

In general, the studied PILs showed thermal stabilities in the range of approximately 25 to 90 °C. For the analyses of the PILs, it was observed that the T_d increased as the substitution of the cation increased in the N, which corresponded to a greater thermal stability for the NTBA. Greater thermal stability means that there is a lower amount of free precursor species of PILs in the autoprotolysis equilibrium.

The TGA profiles of the studied PILs indicate a one-step decomposition temperature for all ammonium-based PILs, except for NEA. In this case, it is a two-stage decomposition. In the first stage, about 10% decomposed at 93.94 °C and the other 90% disappeared at 300 °C in the second stage.

3.4. Correlations

T_d vs. ΔpK_a and pK_a

We can analyze the physicochemical properties in terms of changes in the ΔpK_a of PILs. The PILs with a low ΔpK_a indicate that free acids and bases are present in the system. In this sense, to understand the physicochemical properties and the behavior of these PILs, we could analyze the relationship between the experimental weight loss that indicates their thermal stability and the changes in ΔpK_a for the MeOH and DMSO solvents. Special emphasis was given to the degree of proton transfer and thermal stability depending on

the change in the ΔpK_a . Additionally, we were able to compare the previous parameters with the pK_a data that were previously determined with the indicator method.

It is interesting to observe the relationship between the different parameters that are obtained, in order to compare the information that they provide on the state of the PILs that are studied in the molecular solvents MeOH and DMSO. For this, these parameters are plotted and shown in Figure 6.

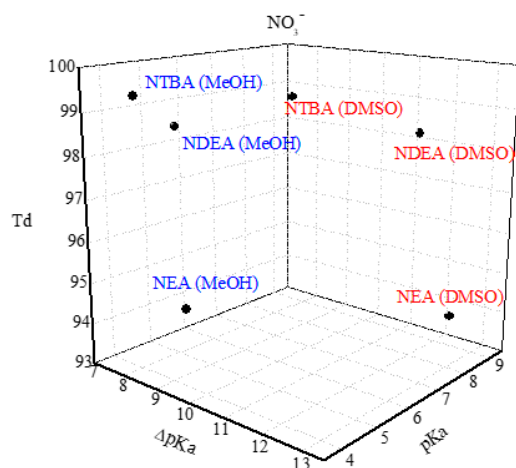


Figure 6. Variation of pK_a , ΔpK_a and T_d values for the PILs analyzed.

Figure 6 shows the NTBA with a higher T_d , indicating greater thermal stability; therefore, in the pure state, they would present negligible amounts of free precursor species corresponding to a high ionic character. However, when PILs are found in molar concentrations in molecular solvents, their autoprotolysis equilibrium is affected by the nature of the molecular solvent and its acid-base properties by free precursor species, resulting in more basic or more acidic global systems. This can be seen in their pK_a values, which are lower in MeOH in relation to DMSO. For this reason, we observed a marked solvent effect on the ionization of PILs, where the highest values of ΔpK_a or higher ionic character were conditioned with high values of pK_a ($\Delta pK_a^{DMSO} > \Delta pK_a^{MeOH}$ y $pK_a^{DMSO} > pK_a^{MeOH}$)).

4. Conclusions

For the range of molar fractions from $x_{PIL} \sim 0.2$ to 1, no considerable changes are observed in the spectrum of sensor I. This may indicate that the ionic lattice is organized, and as a consequence, the effect of the molecular solvent and therefore its solvation effect is negligible. For the range of molar concentration, we observed the protonation of indicator I by the acidic species that were the precursor of the PILs in each solvent. On the other hand, an increment in the capacity of the molecular solvent HBD resulted in an increment in the acidity of the PILs, while showing a weak cation–anion interaction, and the proton being more available for solvation.

High ΔpK_a values ensure a PIL with a high ion pair character in DMSO, while the opposite is observed in MeOH. This agrees with the reported values of pK_a^{PILs} that are determined by the indicator method [21], where an increment in the H-bonding capacity of the molecular solvent results in a decrease in these values. For the pure PILs, it was observed that T_d increased as the substitution in the N of the cation increased, which corresponded to a greater thermal stability for NTBA, being mainly found as an ionic pair. This was consistent with what was determined by cyclic voltammetry, where no neutral free species were detected for this PIL. However, in diluted solutions, the effect of molecular solvents in the solvation process for NTBA is evidenced, presenting the highest acidity values.

Author Contributions: C.G.A. is the director of the research project that funds this work. She is the researcher responsible and actually she works in the design of the synthesis of ionic liquids for its use in different applications. She has also carried out different investigations in the study of solvent and solvatochromic probes. M.V.B. has researched the design and synthesis of ionic liquids, as well as solvent studies and solvatochromic indicators. Currently she is working on modified β -cyclodextrins with ionic liquids. L.G. is working with a scientific initiation scholarship in our group. All authors have read and agreed to the published version of the manuscript.

Funding: This research was funded by Research and Development Project: “New ionic materials on the structural basis of ionic liquids. Synthesis and characterization. Application to various physicochemical processes”. CAI+D. PIC-UNL. From 02-2021 to 02-2023. Project No 50620190100106LI. Amount \$180,000 Director: Dr. Claudia G. Adam. Co-Director: Dr. Graciela Fortunato.

Institutional Review Board Statement: Not applicable.

Informed Consent Statement: Not applicable.

Data Availability Statement: Not applicable.

Conflicts of Interest: The authors declare no conflict of interest.

References

1. Picquet, M.; Tkatchenko, I.; Tommasi, I.; Wasserscheid, P.; Zimmermann, J. Ionic liquids, 3. Synthesis and utilization of protic imidazolium salts in homogeneous catalysis. *Adv. Synth. Catal.* **2003**, *345*, 959–962. [[CrossRef](#)]
2. Qiao, Y.; Hou, Z.; Li, H.; Hu, Y.; Feng, B.; Wang, X.; Hua, L.; Huang, Q. Polyoxometalate-based protic alkylimidazolium salts as reaction-induced phase-separation catalysts for olefin epoxidation. *Green Chem.* **2009**, *11*, 1955–1960. [[CrossRef](#)]
3. Adam, C.G.; Fortunato, G.G.; Mancini, P.M.J. Nucleophilic and acid catalyst behavior of a protic ionic liquid in a molecular reaction media. Part 1. *Phys. Org. Chem.* **2009**, *22*, 460–465. [[CrossRef](#)]
4. Han, X.; Armstrong, D.W. Ionic liquids in separations. *Acc. Chem. Res.* **2007**, *40*, 1079–1086. [[CrossRef](#)] [[PubMed](#)]
5. Qin, Y.; Lu, X.; Sun, N.; Rogers, R.D. Dissolution or extraction of crustacean shells using ionic liquids to obtain high molecular weight purified chitin and direct production of chitin films and fibers. *Green Chem.* **2010**, *12*, 968–971. [[CrossRef](#)]
6. Tan, S.S.Y.; MacFarlane, D.R.; Upfal, J.; Edye, L.A.; Doherty, W.O.S.; Patti, A.F.; Pringle, J.M.; Scott, J.L. Extraction of lignin from lignocellulose at atmospheric pressure using alkylbenzenesulfonate ionic liquid. *Green Chem.* **2009**, *11*, 339–345. [[CrossRef](#)]
7. Timperman, L.; Skowron, P.; Boisset, A.; Galiano, H.; Lemordant, D.; Frackowiak, E.; Beguin, F.; Anouti, M. Triethylammonium bis(tetrafluoromethylsulfonyl)amide protic ionic liquid as an electrolyte for electrical double-layer capacitors. *Phys. Chem. Chem. Phys.* **2012**, *14*, 8199–8207. [[CrossRef](#)]
8. Anouti, M.; Timperman, L. A pyrrolidinium nitrate protic ionic liquid-based electrolyte for very low-temperature electrical doublelayer capacitors. *Phys. Chem. Chem. Phys.* **2013**, *15*, 6539–6548. [[CrossRef](#)]
9. Menne, S.; Pires, J.; Anouti, M.; Balducci, A. Protic ionic liquids as electrolytes for lithium-ion batteries. *Electrochem. Commun.* **2013**, *31*, 39–41. [[CrossRef](#)]
10. Li, S.; Banuelos, J.L.; Zhang, P.; Feng, G.; Dai, S.; Rother, G.; Cummings, P.T. Toward understanding the structural heterogeneity and ion pair stability in dicationic ionic liquids. *Soft Matter* **2014**, *10*, 9193–9200. [[CrossRef](#)]
11. Armand, M.; Endres, F.; MacFarlane, D.R.; Ohno, H.; Scrosati, B. Ionic liquid materials for the electrochemical challenges of the future. *Nat. Mater.* **2009**, *8*, 621–629. [[CrossRef](#)] [[PubMed](#)]
12. Le Bideau, J.L.; Viau, L.; Vioux, A. Ionogels, ionic liquid based hybrid materials. *Chem. Soc. Rev.* **2011**, *40*, 907–925. [[CrossRef](#)] [[PubMed](#)]
13. Nuthakki, B.; Greaves, T.L.; Krodziewska, I.; Weerawardena, A.; Burgar, M.I.; Mulder, R.J.; Drummond, C.J. Protic ionic liquids and ionicity. *Aust. J. Chem.* **2007**, *60*, 21–28. [[CrossRef](#)]
14. Greaves, T.L.; Drummond, C.J. Protic ionic liquids: Properties and applications. *Chem. Rev.* **2008**, *108*, 206–237. [[CrossRef](#)]
15. Fumino, K.; Poppel, T.; Geppert-Rybczynska, M.; Zaitsau, D.H.; Lehmann, J.K.; Verevkin, S.P.; Kockerling, M.; Ludwig, R. The influence of hydrogen bonding on the physical properties of ionic liquids. *Phys. Chem. Chem. Phys.* **2011**, *13*, 14064–14075. [[CrossRef](#)]
16. Dong, K.; Zhang, S.; Wang, J. Understanding the hydrogen bonds in ionic liquids and their roles in properties and reactions. *Chem. Commun.* **2016**, *52*, 6744–6764. [[CrossRef](#)]
17. Dong, K.; Zhang, S. Hydrogen bonds: A structural insight into ionic liquids. *Chem. Eur. J.* **2012**, *18*, 2748–2761. [[CrossRef](#)]
18. Bravo, M.V.; Fernández, J.L.; Adam, C.G.; Della Rosa, C.D. Understanding the Role of Protic Ionic Liquids (PILs) in Reactive Systems: Rational Selection of PILs for the Design of Green Synthesis Strategies for Allylic Amines and β -Amino Esters. *ChemPlusChem* **2019**, *84*, 919–926. [[CrossRef](#)]
19. Fortunato, G.G.; Mancini, P.M.; Bravo, M.V.; Adam, C. New Solvents Designed on the Basis of the Molecular-Microscopic Properties of Binary Mixtures of the Type (Protic Molecular Solvent + 1-Butyl-3-methylimidazolium-Based Ionic Liquid). *J. Phys. Chem. B* **2010**, *114*, 11804–11819. [[CrossRef](#)]

20. Chen, K.; Wang, Y.; Yao, J.; Li, H. Equilibrium in Protic Ionic Liquids: The Degree of Proton Transfer and Thermodynamic Properties. *J. Phys. Chem. B* **2018**, *122*, 309–315. [[CrossRef](#)]
21. Adam, C.G.; Bravo, M.V.; Mancini, P.M.E. Molecular solvent effect on the acidity constant of protic ionic liquids. *Tetrahedron Lett.* **2014**, *55*, 148–150. [[CrossRef](#)]
22. Mancini, P.M.; Adam, C.; Pérez, A.; Vottero, L.R. Solvatochromism in binary solvent mixtures. Response models to the chemical properties of reference probes. *J. Phys. Org. Chem.* **2000**, *13*, 221. [[CrossRef](#)]
23. Reichardt, C. Polarity of ionic liquids determined empirically by means of solvatochromic pyridinium N-phenolate betaine dyes. *Royal Soc. Chem. Green Chem.* **2005**, *7*, 339. [[CrossRef](#)]
24. Muhammed, S.M.; Hiroshi, K.; Tomohiro, Y.; Md Abu Bin Hasan, S.; Masayoshi, W. Physicochemical properties determined by ΔpK_a for protic ionic liquids based on an organic super-strong base with various Brønsted acids. *Phys. Chem. Chem. Phys.* **2012**, *14*, 5178–5186.
25. Ullah, Z.; Bustam, M.A.; Man, Z.; Khan, A.S. Thermal stability and kinetic study of benzimidazolium based ionic liquid. *Procedia Eng.* **2016**, *148*, 215–222. [[CrossRef](#)]
26. Zailani, N.H.Z.; Yunus, N.M.; Rahim, A.H.; Bustam, M.A. Thermophysical Properties of Newly Synthesized Ammonium-Based Protic Ionic Liquids: Effect of Temperature, Anion and Alkyl Chain Length. *Processes* **2020**, *8*, 742. [[CrossRef](#)]
27. Elshereksi, N.W.; Mohamed, S.M.; Arifin, A.; Ishak, Z.A.M. Thermal Characterisation of Poly(Methyl Methacrylate) Filled with Barium Titanate as Denture Base Material. *J. Phys. Sci.* **2014**, *25*, 15–27.
28. Kaczmarek, P.G.J.K.H. Thermogravimetric analysis of thermal stability of poly(methylmethacrylate) films modified with photoinitiators. *Therm. Anal. Calorim.* **2014**, *115*, 1387–1394. [[CrossRef](#)]
29. Sivakumar, M.; Panduranga Rao, K. Synthesis and characterization of poly(methyl methacrylate) functional microspheres. *React. Funct. Polym.* **2000**, *46*, 29–37. [[CrossRef](#)]
30. Yoshizawa, M.; Xu, W.; Austen Angell, C. Ionic liquids by proton transfer: Vapor pressure, conductivity, and the relevance of ΔpK_a from aqueous solutions. *J. Am. Chem. Soc.* **2003**, *125*, 15411. [[CrossRef](#)]
31. Stoimenovski, J.; Izgorodina, E.I.; MacFarlane, D.R. Ionicity and proton transfer in protic ionic liquids. *Phys. Chem. Chem. Phys.* **2010**, *12*, 10341. [[CrossRef](#)] [[PubMed](#)]
32. Tokuda, H.; Hayamizu, K.; Ishii, K.; Susan, M.A.B.H.; Watanabe, M. Physicochemical Properties and Structures of Room Temperature Ionic Liquids. 1. Variation of Anionic Species. *J. Phys. Chem. B* **2004**, *108*, 16593. [[CrossRef](#)]
33. De Ligny, C.L. The dissociation constants of some aliphatic amines in water and methanol-water mixtures at 25. *Recueil Travaux Chimiques Pays-Bas. Utrecht* **1959**, *79*, 731–736. [[CrossRef](#)]
34. Miguel, E.L.M.; Silva, P.L.; Pliego, J.R. Theoretical Prediction of pKa in Methanol: Testing SM8 and SMD Models for Carboxylic Acids, Phenols, and Amines. *J. Phys. Chem. B* **2014**, *118*, 5730–5739. [[CrossRef](#)]
35. Rived, F.; Canals, I.; Bosch, E.; Rosés, M. Acidity in methanol–water. *Anal. Chim. Acta* **2001**, *439*, 315–333. [[CrossRef](#)]
36. Rived, F.; Canals, I.; Bosch, E.; Rosés, M. Dissociation constants of neutral and charged acids in methyl alcohol. The acid strength resolution. *Anal. Chim. Acta* **1998**, *374*, 309–324. [[CrossRef](#)]
37. Tshepelevitsh, S.; Kütt, A.; Lõkov, M.; Kaljurand, I.; Saame, J.; Heering, A.; Plioger, P.; Vianello, R.; Leito, I. On the Basicity of Organic Bases in Different Media. *Eur. J. Org. Chem.* **2019**, *2019*, 1–22. [[CrossRef](#)]
38. Wu, F.; Xiang, J.; Chen, R.; Li, L.; Chen, J.; Chen, S. Physicochemical properties determined by ΔpK_a for protic ionic liquids based on an organic super-strong base with various Brønsted acids. *J. Phys. Chem. C* **2010**, *114*, 20007. [[CrossRef](#)]
39. Bautista-Martinez, J.A.; Tang, L.; Belieres, J.-P.; Zeller, R.; Angell, C.A.; Friesen, C. Hydrogen redox in protic ionic liquids and a direct measurement of proton thermodynamics. *J. Phys. Chem. C* **2009**, *113*, 12586. [[CrossRef](#)]
40. Anouti, M.; Caillon-Caravian, M.; Le Flock, C.; Lemordant, D. Alkylammonium-Based Protic Ionic Liquids. II. Ionic Transport and Heat-Transfer Properties: Fragility and Ionicity Rule. *J. Phys. Chem. B* **2008**, *112*, 31–9412. [[CrossRef](#)]
41. Ueno, K.; Tokuda, H.; Watanabe, M. Ionicity in ionic liquids: Correlation with ionic structure and physicochemical properties. *Phys. Chem. Chem. Phys.* **2010**, *12*, 1649. [[CrossRef](#)] [[PubMed](#)]
42. Tokuda, H.; Hayamizu, K.; Ishii, K.; Susan, M.A.B.H.; Watanabe, M. Physicochemical Properties and Structures of Room Temperature Ionic Liquids. 2. Variation of Alkyl Chain Length in Imidazolium Cation. *J. Phys. Chem. B* **2005**, *109*, 6103. [[CrossRef](#)] [[PubMed](#)]
43. Tokuda, H.; Ishii, K.; Susan, M.A.B.H.; Tsuzuki, S.; Hayamizu, K.; Watanabe, M. Physicochemical Properties and Structures of Room-Temperature Ionic Liquids. 3. Variation of Cationic Structures. *J. Phys. Chem. B* **2006**, *110*, 2833. [[CrossRef](#)] [[PubMed](#)]
44. Tokuda, H.; Tsuzuki, S.; Susan, M.A.B.H.; Hayamizu, K.; Watanabe, M. How Ionic Are Room-Temperature Ionic Liquids? An Indicator of the Physicochemical Properties. *J. Phys. Chem. B* **2006**, *110*, 39–19593. [[CrossRef](#)]
45. Miran, M.S.; Kinoshita, H.; Yasuda, T.; Susan, M.A.B.H.; Watanabe, M. Hydrogen bonds in protic ionic liquids and their correlation with physicochemical properties. *Chem. Commun.* **2011**, *47*, 12676. [[CrossRef](#)]
46. Chennuri, B.K.; Gardas, R.L. Measurement and correlation for the thermophysical properties of hydroxyethyl ammonium based protic ionic liquids: Effect of temperature and alkyl chain length on anion. *Fluid Phase Equilibria* **2016**, *427*, 282–290. [[CrossRef](#)]